Science of the Total Environment 935 (2024) 173262

Contents lists available at ScienceDirect

Science of the Total Environment

journal homepage: www.elsevier.com/locate/scitotenv

Review

Towards solving the reproducibility crisis in surface-enhanced Raman spectroscopy-based pesticide detection

Andrey Averkiev [a], Raul D. Rodriguez [a,*], Maxim Fatkullin [a], Anna Lipovka [a], Bin Yang [b], Xin Jia [b,*], Olfa Kanoun [c], Evgeniya Sheremet [a]

[a] Tomsk Polytechnic University, Lenina ave. 30, Tomsk, Russia
[b] School of Chemistry and Chemical Engineering/State Key Laboratory Incubation Base for Green Processing of Chemical Engineering, Shihezi University, Shihezi, Xinjiang 832003, China
[c] Professorship of Measurement and Sensor Technology, Chemnitz University of Technology, Chemnitz 09126, Germany

HIGHLIGHTS

- SERS holds a promise for rapid, selective, sensitive onsite pesticide detection.
- Reported Raman spectra of malathion, chlorpyrifos, imidacloprid are very consistent.
- Reported SERS spectra of the same pesticides are extremely variable.
- SERS spectra variability can be explained by multiple mechanisms.
- Systematic approach is needed to achieve analytical standards.

GRAPHICAL ABSTRACT

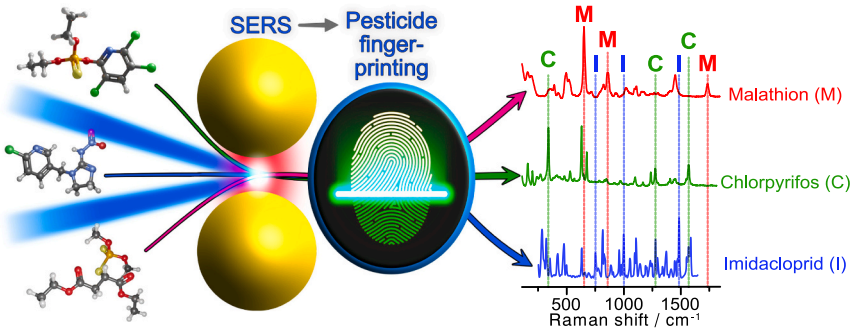

ARTICLE INFO

Editor: Yolanda Picó

Keywords:
Pesticides detection
SERS
Raman spectroscopy
Malathion
Chlorpyrifos
Imidacloprid

ABSTRACT

Growing concerns about pesticide residues in agriculture are pushing the scientific community to develop innovative and efficient methods for detecting these substances at low concentrations down to the molecular level. In this context, surface-enhanced Raman spectroscopy (SERS) is a powerful analytical method that has so far already undergone some validation for its effectiveness in pesticide detection. However, despite its great potential, SERS faces significant difficulties obtaining reproducible and accurate pesticide spectra, particularly for some of the most widely used pesticides, such as malathion, chlorpyrifos, and imidacloprid. Those inconsistencies can be attributed to several factors, such as interactions between pesticides and SERS substrates and the variety of substrates and solvents used. In addition, differences in the equipment used to obtain SERS spectra and the lack of standards for control experiments further complicate the reproducibility and reliability of SERS data. This review systematically discusses the problems mentioned above, including a comprehensive analysis of the challenges in precisely evaluating SERS spectra for pesticide detection. We not only point out the existing limitations of the method, which can be traced in previous review works, but also offer practical recommendations to improve the quality and comparability of SERS spectra, thereby expanding the potential applications of the method in such an essential field as pesticide detection.

* Corresponding authors.
E-mail addresses: raul@tpu.ru (R.D. Rodriguez), jiaxin@shzu.edu.cn (X. Jia).

https://doi.org/10.1016/j.scitotenv.2024.173262
Received 25 January 2024; Received in revised form 8 May 2024; Accepted 13 May 2024
Available online 18 May 2024

1. Introduction

Over the past century, pesticides have become nearly indispensable in agriculture, significantly increasing crop yields and global food production (Alexandratos et al., 2012; Carvalho, 2017). While these chemicals are crucial in achieving sustainable food production, their use has serious negative consequences for public health and the environment. Unintentional pesticide intake leads to approximately 355,000 deaths annually worldwide (Alavanja, 2009; Alavanja and Bonner, 2012). Most of these incidents result from overexposure and misuse of these toxic substances. However, pesticides also tend to accumulate in crops, disperse through the air, and settle in soil and water. These harmful substances can travel long distances and become sources of environmental pollution (Qu et al., 2019).

Considering the rising concerns about the pesticide content in food and drinks, we must establish reliable quality control and develop sensitive methods to detect pesticide residues. The widely implemented rapid detection methods for these purposes include enzyme-linked immunosorbent assay (ELISA) (Narenderan et al., 2020), and lateral flow immunoassay (LFIA) (Wang et al., 2014). LFIA offers several advantages, including ease of use, fast analysis, low cost, and high-throughput screening for multiple target analytes (Chen et al., 2017). In addition to LFIA and biochip microarray-based assays, ELISA and fluorescence-linked immunosorbent assay (FLISA) enable quantitative analysis for each analyte using multiple-label strategies (Song et al., 2015; Yu et al., 2018). Multiplexed antibody-based assays enable high-throughput, high-efficiency, rapid, and quantitative assays. Additionally, near-infrared (NIR) spectroscopy techniques are recognized as non-destructive evaluation methods for quality control of intact food products (Nazarloo et al., 2021).

In recent years, surface-enhanced Raman spectroscopy (SERS) has gained increasing attention as an advanced analytical method for pesticide detection. By amplifying Raman scattering signals, SERS provides a highly sensitive, accessible, and selective approach for detecting various analytes, including pesticides (Kaur et al., 2021; Tsagkaris et al., 2021). SERS would be preferred when rapid, selective, and highly sensitive onsite detection of pesticides is required without the need for complicated experimental setup or strict sample preparation conditions. Furthermore, SERS enables multiplex analysis for the simultaneous detection of multiple pesticides. The typical substrate choice for these purposes is based on plasmonic structures, which could be further enhanced by incorporating specific ligands or receptors, facilitating the selective binding and detection of several pesticide molecules in a single experiment (Jiang et al., 2021; Xu et al., 2023; C. Liu et al., 2022; Zhang et al., 2021).

Despite all the potential advantages, interpreting SERS spectra and standardizing experimental procedures pose significant challenges. This mini-review aims to highlight the issues in interpreting and analyzing pesticide SERS spectra, identify the gaps in current methodologies, and propose strategies for enhancing the quality and efficiency of research in this evolving domain.

To provide a more in-depth and meaningful analysis, we discuss the issues of SERS detection of the three most commonly used pesticides: malathion, chlorpyrifos, and imidacloprid. These pesticides represent different groups of insecticides, such as neonicotinoids (imidacloprid) and organophosphate (malathion and chlorpyrifos). Moreover, all selected pesticides are systemic, meaning their detection is critical since they could penetrate the treated crop. Their distinct chemical structures define the different interactions with noble metal SERS substrates that would affect SERS spectra. For instance, sulfur-containing malathion and chlorpyrifos are expected to have a good affinity towards SERS substrates, while sulfur-free imidacloprid would interact differently. On the other hand, chlorpyrifos and imidacloprid have chlorine atoms, which also could accelerate and enhance adsorption processes. To sum up, we chose only three pesticides for analysis to represent different molecule-substrate interactions and associated problems in SERS detection while providing a detailed analysis of the spectra and experimental conditions.

Several review articles are currently dedicated to pesticide detection using SERS (Kulakovich et al., 2022; Lin and He, 2019; C. Liu et al., 2022; Pang et al., 2016). These works showcase some of the latest developments in the field and explore potential applications in food safety or agricultural security (Moldovan et al., 2021; Xu et al., 2017). In contrast to those previous reviews, our mini-review focuses specifically on the current challenges associated with SERS-based detection of pesticides. In particular, we address the issues of reproducibility, validation, and standardization of the spectra. While other works mainly focus on the advantages of SERS, we believe it is essential to reveal its blind spots and discuss how to overcome them. That goal is the core of this review article.

2. Reported results

Malathion, chlorpyrifos, and imidacloprid are some of the most extensively used insecticides worldwide (Bakirhan et al., 2018; Richendrfer and Creton, 2015; Valdovinos-Flores et al., 2017; Wu et al., 2011). To set a reference point, before analyzing SERS, it is necessary first to describe the classical Raman spectra of each pesticide. These data are well-established in scientific literature.

Malathion, an organophosphorus compound extensively used as an insecticide and acaricide, has an established permissible level of 0.1 μg/L (0.3 nM) set by the World Health Organization (WHO) (Vasseghian et al., 2022). Its Raman spectra are notably consistent across various studies, displaying a characteristic pattern as illustrated in Fig. 1a (Liu and Liu, 2011). This spectrum, with minor variations, has been replicated in other research works (Asgari et al., 2021; Fathi et al., 2012; Quintás et al., 2004).

Chlorpyrifos, another widely used organophosphorus pesticide in agriculture, has a permissible level of 0.1 part per million (ppm) or ~ 0.01 mg/L (28.5 nM), according to the WHO (Zhu et al., 2019). Its Raman spectra are well-documented and display a distinct structure, as depicted in Fig. 1b (Liu and Liu, 2011), and have been consistently reproduced in several publications (Li et al., 2012; Ma et al., 2020; Ngo et al., 2020; Zhu et al., 2018).

Lastly, **imidacloprid**, an insecticide known for its frequent use as a model for pesticide residue detection and agricultural quality control, has a maximum permissible level of 1.05 μg/L (3.18 nM) as determined by the United States Environmental Protection Agency (Starner and Goh, 2012). The typical Raman spectrum of imidacloprid is shown in Fig. 1c (Abu Bakar and Shapter, 2023). This spectral pattern, with the largest number of peaks compared to the pesticide above, has been consistently observed in many studies, supporting its reproducibility and reliability (Creedon et al., 2020; Dias et al., 2019; Liang et al., 2022).

In Fig. 1d, we show the Raman spectra of these pesticides plotted together in a single graph, complemented by the peak assignments summarized in Table 1. We marked at least three peaks characteristic of each molecule that had the least overlap with the others to facilitate their identification in pesticide mixtures. Each of these pesticides belongs to a distinct chemical group, significantly influencing their solubility and adsorption characteristics on various substrates. This diversity reflects the challenges that our study aims to address. In the following sections, we highlight the issues that arise in SERS but not in Raman and present a detailed analysis for each pesticide.

The reports discussed in this mini-review were selected according to the following criteria: 1) the presence of SERS spectra of malathion, chlorpyrifos, or imidacloprid, and 2) the use of SERS substrates made of noble metals. To our knowledge, this selection is complete up to the submission date.

3. Shifting from Raman to SERS: the complications in pesticide detection

While conventional Raman spectra for the selected pesticides tend to be relatively consistent and well-documented in literature and databases, SERS often presents much less predictable results, limiting its chances of being widely applied. In an ideal situation, pesticide molecules would bind to the "hot spots" on the substrate—sites with highly enhanced electromagnetic (EM) fields—leading to intense and highly specific signals. In reality, observed peaks may not resemble the Raman spectra or vastly vary in experiments performed by different groups, as shown in this mini-review. The potential reasons for this are the state of the sample, substrate reproducibility, their interactions, and other experimental conditions.

Sample preparation within the discussed works needs to be unified since they are typically prepared using different solvents (like ethanol, methanol, or water) or matrices (like tea leaves or tomatoes), using various procedures (whether in liquid or dry states). Pesticide's purity also may vary. The solvents, matrices, and contaminants may lead to the non-specific binding of molecules that are not the intended target. This phenomenon often prevents the reproducibility of results, potentially causing misestimation of the actual pesticide concentration or misinterpretation of its presence. This issue is partly caused by the limited availability of surface sites on the SERS substrates to bind specific capture agents. Such nonspecific interactions tend to increase background noise and reduce the specificity of labeling, leading to inaccuracies in interpreting the SERS spectra (Bernat et al., 2019).

SERS substrate reproducibility is another well-known issue the scientific community seeks to solve. There are problems related to "hot spots" homogeneity, multiplex detection capability, and sensitivity of SERS substrates (Fan et al., 2020; Liu et al., 2021; Mosier-Boss, 2017; Ouyang et al., 2017). Previously, the SERS substrate material was believed to heavily influence the resulting spectra due to metal-dependent chemical (CM) enhancement and localized surface plasmon resonance (LSPR) conditions. However, later research works show that

Table 1
Raman peak assignments for malathion, chlorpyrifos, and imidacloprid.

Pesticide	Raman shift (cm^{-1})
Malathion	159 (P—O vibration)
	496 (P—S vibration)
	652 (P═S vibration)
	859 (C-O-C stretching)
	1022 (C—H in plane)
	1110 (C—C stretching)
	1451 (CH_2 deformation)
	1733 (C═O stretching)
	2800 (CH_3 deformation)
	3100 (C—H stretching)
Chlorpyrifos	158 (P—O vibration)
	340 (N–cyclopropyl)
	530 (P—O stretching)
	630 (Ring deformation)
	676 (Ring breathing)
	1100 (P-O-C vibration)
	1238 (ring mode or Cl—H stretching)
	1276 (C—H bending)
	1447 (Cl-ring and C═C stretching)
	1569 (C═C stretching)
	2800 (C—H stretching)
	3100 (C—H stretching)
Imidacloprid	283 (—H rocking, C—Cl bending)
	322 (C—N wagging, C—N bending)
	476 (C—N bending/rocking, C—Cl stretching, C—C wagging)
	633 (C—N bending, C—C bending)
	751 (N–O/C–N bending, C—C stretching, C—H rocking)
	816 (C—N bending, C–C/C–Cl stretching, C—H rocking)
	999 (C—N bending)
	1109 (C—H bending, C—Cl stretching)
	1277 (C—C bending, C—H wagging)
	1371 (C–C/C–N stretching)
	1483 (C—H bending)
	1583 (C—C stretching)

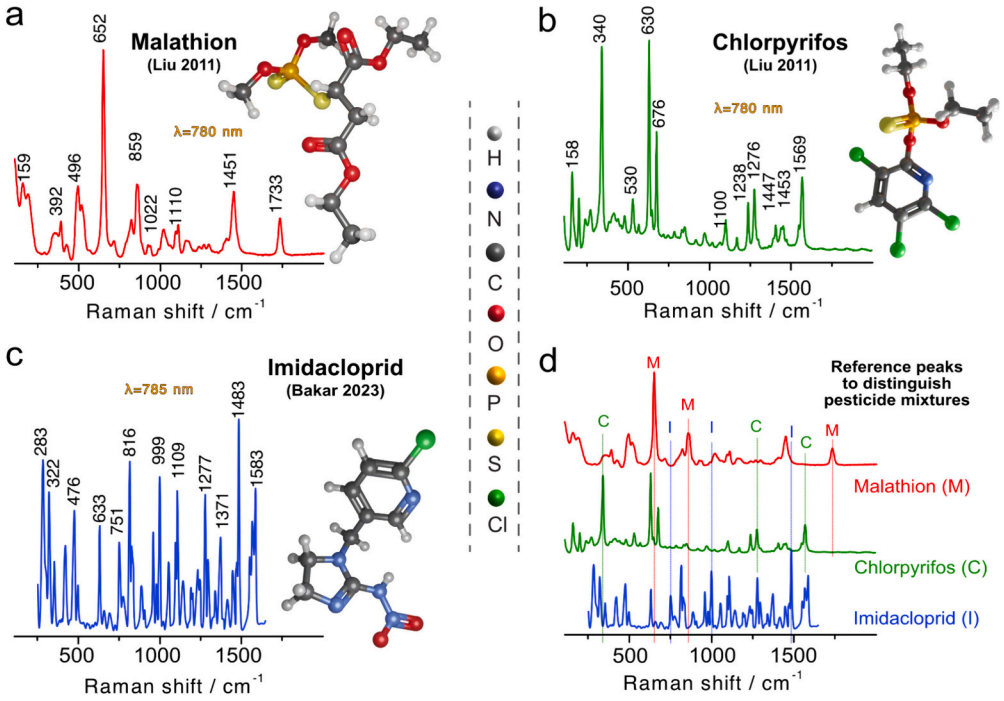

Fig. 1. Conventional (non-enhanced) Raman spectra of pesticides: a) malathion (Liu and Liu, 2011), b) chlorpyrifos (Liu and Liu, 2011), and c) imidacloprid (Abu Bakar and Shapter, 2023). The molecular structure of each pesticide is shown as insets. d) Raman spectra of malathion, chlorpyrifos, and imidacloprid in a single graph. The peak positions are marked as M, C, and I, respectively, to indicate the most suitable peaks for distinguishing these pesticides. Peak assignments are presented in Table 1.

both similar and diverse materials can result in significantly different SERS spectra (Al-Syadi et al., 2021; Chen et al., 2019; Tang et al., 2019; Zhu et al., 2021).

The molecule-substrate interactions also explain the shifts, disappearance, or weakening of the characteristic peaks in SERS compared to the pesticide standard Raman spectra. Additionally, there needs to be more comprehensive peak descriptions in SERS research, with many studies only discussing a few characteristic peaks and omitting others. The complexity of different enhancement mechanisms and the high sensitivity of SERS also make it susceptible to artifacts. The variability in research methodologies further complicates the signal interpretation. Diverse choices in substrates, equipment, experimental setups, and solvents used in different studies lead to variations in binding behaviors and even chemical reactions, creating new compounds that are challenging to consistently interpret and compare (Pang et al., 2016).

Further, we will discuss the reported SERS data for each pesticide, highlighting the particular challenges and limitations for each case. The specific measurement conditions, assigned peaks, and methodological and analytical details are provided in Table S1 in Supplementary Information.

3.1. Malathion

SERS spectra of malathion were found to vary significantly across different studies, which is attributed to many factors involved in SERS identification. In particular, the choice of SERS substrate affects the possibility of forming new bonds and changing the adsorption geometry of the malathion molecules. Furthermore, pesticide spectra can be derived not only from the pure pesticide or dissolved form but also from pesticide adsorbed on food matrices. This introduces additional changes in the resulting spectrum in the form of the appearance/disappearance of peaks, shifts in peak positions, or changes in their relative intensity.

One of the most significant limitations in malathion analysis is the need to understand why SERS and Raman spectra are that different. In this context, several works failed to clarify the appearance or change of the SERS spectra bands and lack comparison with the Raman spectra reported in the literature. Nie et al. (Nie et al., 2018) developed a label-free aptamer-based SERS sensor specifically for detecting malathion. This sensor was based on silver colloids coated with spermine and aptamer molecules. The malathion molecules were bonded with the aptamer –SH group, followed by mixing with aggregating agents like NaCl, KCl, or $MgCl_2$. The SERS spectra were then recorded using an excitation laser with a wavelength of 633 nm. Researchers identified two main peaks at 1089 and 1270 cm^{-1} corresponding to the P–O–C vibration and P═O stretching, but strangely, the reference cited in that work did not report the peak assignment of the 1270 cm^{-1} band. They observed a shift in the malathion peak from 1089 to 1112 cm^{-1} upon bonding with the aptamer, where the 1112 cm^{-1} peak's relative intensity increased. Although the study briefly mentioned that this shift is connected to the aptamer-malathion interaction, the authors did not discuss the specifics of such spectral changes or provide details on the chemical interactions. Still, that work demonstrated that malathion could be detected at concentrations below 0.165 mg/L (0.5 μM). However, the authors did not compare these malathion SERS or aptamer-bound malathion with standard Raman or other malathion SERS spectra, focusing only on these two peaks for pesticide identification. Unfortunately, the methodology behind assigning these specific peaks to malathion and differentiating it from other molecules was unclear, raising questions about the interpretation of the signal.

Serebrennikova et al. (Serebrennikova et al., 2023) studied the SERS spectra of malathion in ethanol, exploring a concentration range from 0.25 to 50 mg/L, under a 785 nm laser excitation. The researchers reported an innovative SERS substrate using cellulose fiber (CF) modified with silver nanostructures (AgNS). A notable observation from the study was a significant concentration dependence of the 1030 cm^{-1} peak intensity in the SERS spectra. This peak, attributed to P–O–C vibrations, was selected by the authors as the primary marker for the quantitative analysis. Interestingly, the study also included Raman spectra of malathion in ethanol solution as supplementary information, which exhibited differences from the SERS spectra. While the authors identified the three most significant peaks in the Raman spectrum at 895 cm^{-1} (C—C stretching), 1030 cm^{-1} (P–O–C vibrations), and 1050 cm^{-1} (P═O stretching), they did not elaborate on the reasons for the variations observed during SERS detection. Moreover, there was a lack of comparison of these spectra with other reported SERS spectra of malathion. The authors mentioned that the intensity of all characteristic peaks varied with the concentration of the analyte, although a detailed analytical interpretation of these changes could have been useful.

Fathi et al. (Fathi et al., 2012) conducted a detailed Raman and SERS analysis of a malathion solution. However, that work has some limitations regarding the detected species, which were not the original pesticide but its byproducts after hydrolysis in KOH. SERS spectra were acquired after 15 cyclic voltammetry (CV) cycles within a voltage range of 0.5 to 0.9 V versus Ag/AgCl, at a 150 mV s^{-1} scan rate. SERS spectra in this work show distinct stretching modes related to dimethylthiophosphonate. The study assigned characteristic peaks, including 635 cm^{-1} and 685 cm^{-1} (P═S stretching), 815 cm^{-1} (in-phase P–O–C and P—O stretching), 983 cm^{-1} (P—O stretch), 1043 cm^{-1} (P–O–C vibration), 1074 cm^{-1} (out-of-phase P–O–C stretching), 1190 cm^{-1} (P═O stretching), 1342 cm^{-1} (POS^{-} stretching), 1442 cm^{-1} (P–O–CH_3 symmetric stretching), 1505 cm^{-1} (P–O–CH_3 asymmetric stretching), and 1585 cm^{-1} (P–O–S-Ag^{+} complex). Additionally, the authors explained the specific interactions with the Ag substrate, which include the formation of μ–O,S complex bridging between adjacent Ag(I) sites, O, S–chelate, or O– or S–coordinated monodentate complexes, giving insights into the deeper understanding of the processes behind SERS detection.

Asgari et al. (Asgari et al., 2021) developed a specialized SERS microchip equipped with a filtration system for detecting pesticides in fresh produce. The microchip was intricately designed, consisting of five layers: a base glass slide, a lower channel, a filtering membrane, an upper channel, and a top sealing layer of PDMS (polydimethylsiloxane). A solution containing gold and silver nanoparticles (Au@Ag) was introduced into the chip to facilitate SERS signal enhancement. To detect malathion, the pesticide was dissolved in ethanol (with different concentrations) and then applied to a strawberry that had been thoroughly cleaned and cut into pieces. For SERS analysis, these samples were put into ethanol, stirred, and sonicated to extract malathion from the fruit. The SERS analysis of such a mixture was done using a laser at 785 nm wavelength. Going beyond malathion, this study also investigated other pesticides, including thiabendazole, thiram, and endosulfan. However, for malathion, authors focused and discussed only the most prominent band at 1032 cm^{-1} originating from the vibration of the $POCH_3$ groups, and did not discuss the rest of the bands also distinguishable in the spectrum, as depicted in Fig. 2. The study's findings were significant, demonstrating the ability to detect malathion at a limit of detection (LOD) value of less than 100 μg/kg or 0.1 ppm or ~ 0.01 mg/L (30 nM). The authors did not compare their spectra with other published works despite providing separate Raman spectra for all pesticides. What is particularly intriguing is that no noticeable shifts in the analyzed SERS peak were observed when investigating variations in malathion spiked concentration within strawberry extracts. Moreover, there were no indicative peaks of strawberry extract in the spectra. Instead, the only discernible trend was an increase in signal intensity with increasing malathion concentration. The authors acknowledged this phenomenon and highlighted the persistence of characteristic peaks, even in complex sample matrices. This behavior may be attributed to the unique features of the SERS microarray used.

One of the most recent works is the study by Mitra et al. (Mitra et al., 2024), which focuses on the fabrication of SERS-active substrates based on gold nanocolloids impregnated in a matrix of Langmuir–Blodgett (LB) films of MoS_2 flakes. According to the authors, this is the first report

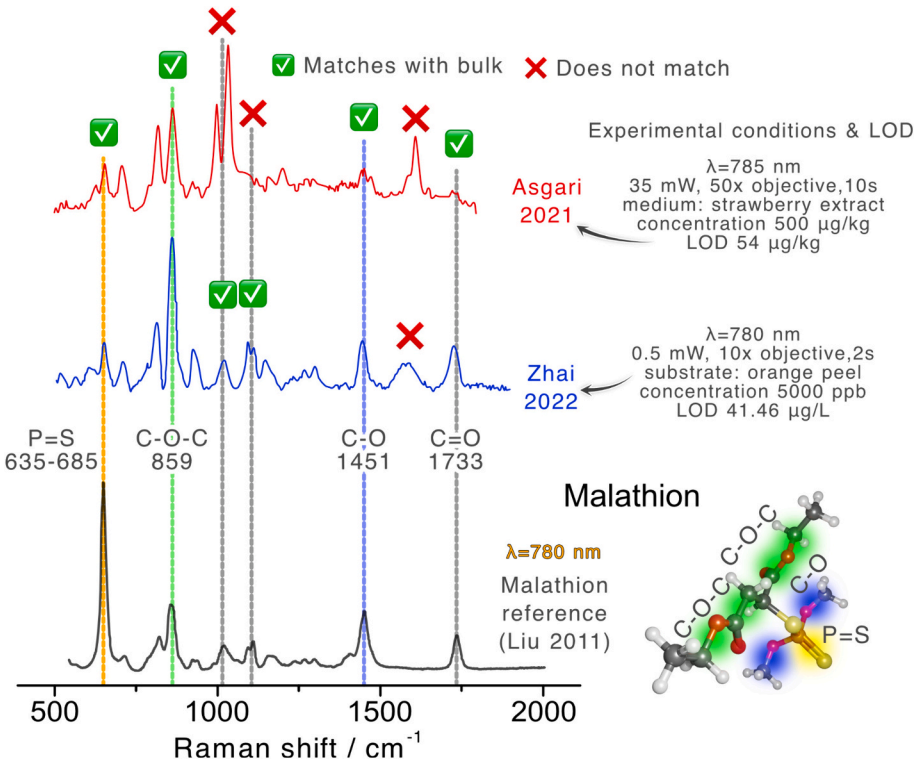

Fig. 2. The most illustrative SERS spectra of malathion with peaks assignment obtained by Asgari et al. (Asgari et al., 2021) and Zhai et al. (Zhai et al., 2022) accompanied by the experimental details and LODs. The spectra are compared to the reference Raman spectrum from Liu et al. (Liu and Liu, 2011) to illustrate the matches and mismatches in characteristic peaks.

where gold nanoparticle and MoS_2 LB films are used as a SERS-active platform for trace-level detection of probe molecules and malathion. SERS measurements were performed using a 633 nm wavelength laser (~1 mW power) to detect malathion in aqueous solutions with concentrations ranging from 10^{-7} M to 10^{-12} M.

The authors focused on obtaining and characterizing the SERS substrate and its testing on the benchmark molecule 4–mercaptopyridine (4-Mpy), and provided SERS spectra as a function of malathion concentration. The authors only indicated the characteristic peaks at 438, 740, 819, 1048, 1307, 1429, 1457, 1518, and 1587 cm^{-1} that were labeled on the presented spectra and referred to articles in which the same peaks were indicated. However, there were no peak assignments or discussions on the possible interaction between Au–MoS_2 substrate and malathion molecules studied. In addition, no comparison was made with the existing Raman spectra of malathion in the literature. All of the above factors make it rather difficult to analyze the presented data. Despite the lack of malathion spectra analysis, the authors achieved an LOD of approximately 10^{-13} M, which is well below the standard limits set by WHO, being one of the lowest LODs compared to the state-of-the-art.

While the reports discussed above did not focus on comparing SERS and Raman spectra, some studies demonstrate a deep level of analysis and elaboration on the obtained results. These works not only provide possible explanations for deviations between SERS and Raman spectra but also attribute most characteristic peak variations to specific bond alterations and have control experiments to facilitate comparative analysis. An example of such work is the research conducted by Zhai et al. (Zhai et al., 2022) on the development of a versatile SERS substrate, specifically designed for the rapid and simultaneous detection of multiple pesticides, including malathion, directly on the surface of orange peels. The substrate was constructed by affixing SERS-active silver nanoparticles (AgNPs) onto a chemically modified thin film made of PDMS. The study is notable for its thorough methodology, particularly in detailing the process of obtaining SERS spectra. In addition to malathion, the study successfully reported spectra for two other pesticides, phoxim, and thiram, demonstrating the substrate's capability for multiplexed pesticide detection. For pesticide mixtures, SERS was performed using the transfer of pesticide residues from an orange peel to an AgNPs-PDMS substrate, while for malathion alone, the measurements were performed using an acetonitrile solution apart from fruits. A crucial feature of this work was the presentation of a highly detailed SERS spectrum of malathion obtained using a 780 nm wavelength laser (Fig. 2). This level of detail extended to a comparison with the standard Raman spectrum of malathion, providing a richer context for the SERS data. The authors achieved an LOD for malathion as low as 0.0415 mg/L (12.6 μM).

Moreover, the authors went a step further by identifying specific bond vibrations corresponding to each characteristic peak in the SERS spectra for each of the three pesticides studied. For malathion, these bonds assignment is: 709 cm^{-1} (P═S and P—O stretching); 815 cm^{-1} (C—H out-of-plane bending); 862 cm^{-1} (C–O–C symmetric stretching); 1094 cm^{-1} (C—C stretching); 1144 cm^{-1} (P—S stretching); 1444 cm^{-1} (C—O symmetric stretching); and 1726 cm^{-1}(C═C stretching). It is important to note that the peak assignment made in that work is somewhat different from the rest (see Fig. 2). In other reports, peaks at 815 cm^{-1} and 1043–1090 cm^{-1} range are usually identified as P–O–C modes, peaks in the range 1050–1270 as P═O, and peaks around 1700 cm^{-1} as C═O. A comparative analysis between the Raman and SERS spectra of malathion showed shifts of these peaks, yet they remained clearly identifiable in both spectral forms.

The authors proposed that this distinct arrangement of peaks could be effectively used for the qualitative identification of malathion. However, this study did not compare their Raman/SERS spectra with those reported in the literature. This omission limited the scope for more detailed comparative analyses, which could have provided additional insights into the consistency and specificity of SERS in detecting malathion. Such a comparison is crucial in establishing the reliability and reproducibility of SERS as a pollution diagnostic tool, especially in

complex sample matrices.

To provide a comprehensive overview of the literature and spectral reproducibility, we also include some works that lack sufficient experimental details, such as the excitation wavelength, data about the pesticide used, or control experiments. These data are valuable in illustrating the issue with spectral variation, but one should take care when trying to derive fundamental insight from them.

Benitta et al. (Benitta T et al., 2017) focused on fabricating SERS substrates through two distinct methods: the modified mirror reaction (MMR) and via physical deposition using a silver cluster deposition system (AgNC). The experimental SERS peaks listed in Table S1 were compared with theoretical vibrational frequencies calculated using Density Functional Theory (DFT). The experimental SERS spectra reported in the study show that pinpointing specific peaks could be a significant challenge. This difficulty arises from the identified peak intensities being at the background noise level. While that report provides an extensive account of the methods used to prepare the SERS substrates, it does not provide other critical details like the excitation laser wavelength and the equipment used. Furthermore, the malathion sample preparation during the experiment, such as whether it was in solution or another form, was omitted, creating a gap in the methodology. Additionally, the study does not compare its SERS spectra and identified peaks with those reported in existing SERS/Raman studies. Such a comparison could have provided valuable context and deeper insights, aiding in the interpretation and validation of the findings.

Fig. 2 compares the reported peak positions for the SERS spectra of malathion to the reference Raman spectrum. Among all the works summarized in Table S1, here we selected the SERS spectra that have the closest match with conventional Raman. While the SERS spectra are expected to deviate from the Raman ones, if the general molecular structure is preserved, one would expect a good match with the Raman reports. Otherwise, one might expect a good match between SERS spectra reported in different works, but that does not appear to be the case.

To sum up, malathion must be better represented in the SERS-related literature, with the current literature showing vastly varying peak positions and assignments. Among the few works published, here we want to highlight the works by Zhai et al. (Zhai et al., 2022) and Asgari et al. (Asgari et al., 2021), showing SERS results with a good match with the reference Raman spectrum and comprehensive report and analysis. The results by Fathi et al. (Fathi et al., 2012) are not included in Fig. 2 or Table S1, as the authors detected malathion decomposition products, not the pristine pesticide.

3.2. Chlorpyrifos

There are also some discrepancies in the analysis of chlorpyrifos SERS spectra, the same as for the previous case of malathion. The inconsistencies are mainly attributed to the possible formation of bonds or compounds with silver/gold substrates used to obtain SERS spectra. Moreover, when the pesticide is applied to food samples, the SERS spectra may vary depending on the food matrices used. Finally, the absence of comparisons between SERS and state-of-the-art Raman raises the need to take a more critical look at the results.

We group the analysis of chlorpyrifos SERS spectra depending on the limitations and omissions found in the literature. Thus, the first group of papers needs to contain a sufficient comparison between SERS and Raman. Zhu et al. (Zhu et al., 2019) reported an innovative method for measuring chlorpyrifos residues using SERS, complemented by a unique wavelength selection approach known as interval combination population analysis-minimal redundancy maximal relevance (ICPA–mRMR). The SERS substrate made of Au@Ag nanoparticles was used for chlorpyrifos detection in a water/methanol solution (70,30) under 785 nm excitation. The authors successfully identified several chlorpyrifos characteristic peaks in the SERS spectra, as shown in Fig. 3. These peaks are: 626 cm^{-1} (P═S stretching; 1085 cm^{-1} (P–O–R stretching); 1155 cm^{-1} (C—H deformation); 1260 cm^{-1} (ring mode); 1455 cm^{-1} (C—H deformation); and 1570 cm^{-1} (ring stretching mode). The authors achieved an LOD for chlorpyrifos of 0.035 mg/L (0.1 mM), which is almost five orders of magnitude above the permissible level by WHO. The researchers observed that sulfur-containing pesticides like chlorpyrifos, which contain a P═S bond, demonstrate a strong affinity for metal substrates. This affinity facilitates their SERS detection, as these compounds tend to form covalent bonds with SERS substrates such as Ag—S, Au—S, and Cu—S. However, the study had certain limitations. The authors did not provide references or explanations on how they associated specific bond vibrations with the identified characteristic peaks of the pesticide molecule. Furthermore, there was no direct comparison between the obtained SERS spectra and other Raman or standard SERS spectra of chlorpyrifos. This lack of comparative analysis limits the ability to draw meaningful correlations or contrasts, which could have improved the understanding of the SERS spectra's specificity and sensitivity for chlorpyrifos detection. Such comparisons are crucial in establishing the robustness and reliability of SERS in detecting pesticide residues.

The work of Li et al. (Li et al., 2022) focused on SERS detection of chlorpyrifos and carbendazim, both individually and in a mixture, as well as in real rice samples, using silver nanoflowers (AgNFs) as a substrate. The spectra for various concentrations of chlorpyrifos dissolved in methanol were recorded at a wavelength of 785 nm. The authors identified the most pronounced chlorpyrifos peak at 1282 cm^{-1}, attributed to the ring stretching vibrations within the molecule. They further assigned other observed peaks: 454 cm^{-1} (Cl—H stretching), 537 cm^{-1} (P—O stretching), 565 cm^{-1} (P═S stretching), and several other peaks corresponding to different vibrational modes, as detailed in Fig. 3.

This work is notable for providing a comparative analysis between chlorpyrifos' theoretical and experimental SERS spectra. Most peaks in the experimental spectrum showed slight shifts compared to the theoretical one, though generally aligned. The LOD for chlorpyrifos was determined using Principal Component Analysis (PCA) and was found to be 0.01 mg/L (28.5 nM).

While the study offers an in-depth examination of the distinctive peaks in the spectra, it lacks a discussion on the specifics of how the AgNF-based SERS substrate interacts with chlorpyrifos molecules. Additionally, the authors did not compare their SERS spectra with results from similar studies. Such comparisons could have provided further insights into the specificity and reliability of their SERS method for detecting chlorpyrifos, particularly in relation to the influence of the SERS substrate on the spectral data. This lack of comparative analysis leaves room for further exploration into the nuances of SERS-based detection of chlorpyrifos.

Another category of chlorpyrifos SERS studies shows the need for more explanation or description of the chemical interactions between the SERS substrates and chlorpyrifos molecules. These interactions can significantly affect the intensity and presence/absence of characteristic features of chlorpyrifos molecules in the spectra. For example, in the research by Jia et al. (Jia et al., 2020), SERS nanosensors were explicitly developed for the detection of chlorpyrifos, utilizing a unique method involving drop-casting of sub-micrometer-sized cubic-like plasmonic superparticles (PSPs). The SERS measurements in this study were performed on chlorpyrifos powder dissolved in ethanol using a laser with a wavelength of 758 nm. The authors successfully performed concentration-dependent SERS of chlorpyrifos and identified characteristic Raman bands associated with the pesticide. These bands are 1145 cm^{-1} and 1172 cm^{-1} (ring breathing vibrations), 1230 cm^{-1} (C—H bending), 1268 cm^{-1} (asymmetric C═C stretching), and 1445 cm^{-1} (symmetric C═C stretching). Remarkably, a LOD for trace concentrations of chlorpyrifos was found to be as low as 350 ng/L (1 nM).

The authors observed a notable blue shift of 10 cm^{-1} in all the chlorpyrifos SERS modes, compared to other studies where gold structures were used for SERS. This shift arises from the differences in the

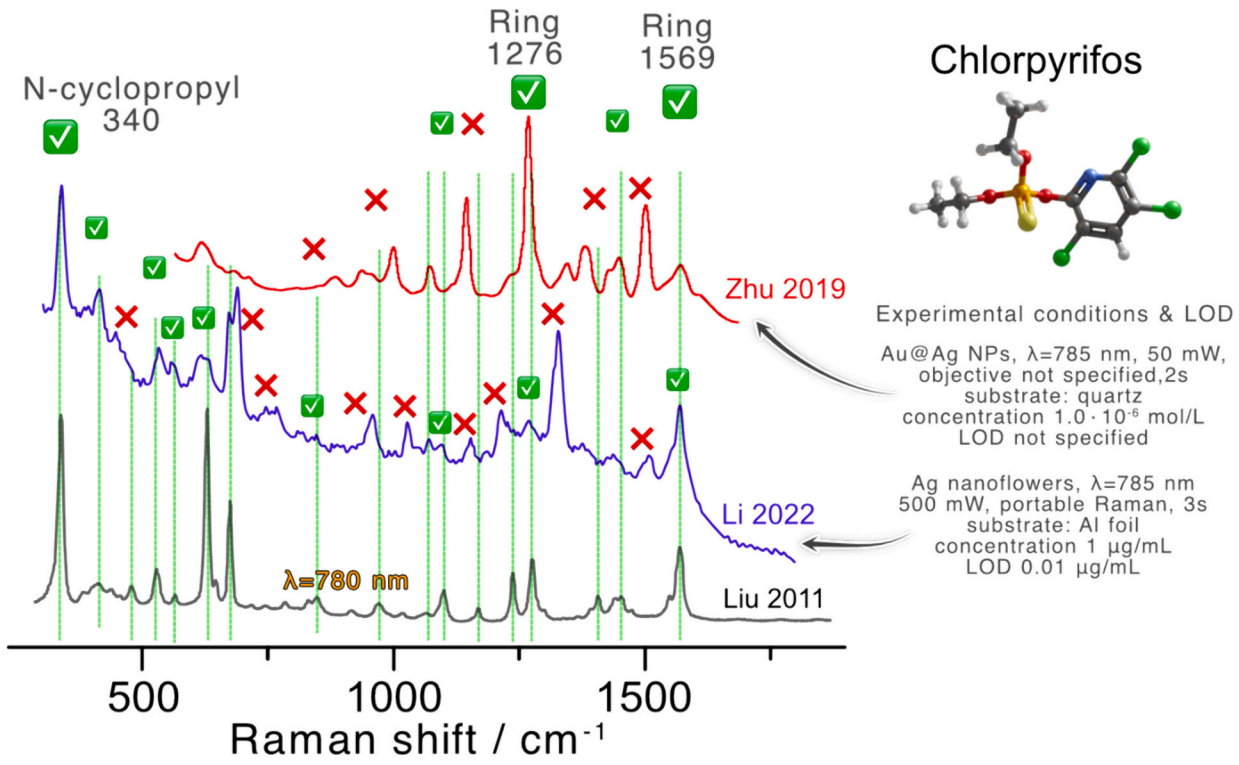

Fig. 3. SERS peaks positions for chlorpyrifos with assignments from the most representative works by Zhu et al. (Zhu et al., 2019) and Li et al. (Li et al., 2022), together with the experimental conditions used in these two works.

interfacial interactions between the silver used in their study and the gold used in other works, both in combination with chlorpyrifos.

An important aspect to consider in this study is the relatively narrow spectral range covered, spanning only approximately 1050 to 1470 cm^{-1}. Typically, chlorpyrifos has distinctive peaks in a broader range. This limitation in the spectral range could overlook other relevant peaks, thereby impacting the comprehensiveness of the analysis. Another ambiguity in this research is the identification of two prominent peaks at 1145 and 1268 cm^{-1} in the SERS data for chlorpyrifos. The study does not provide a direct comparison with conventional Raman spectra of chlorpyrifos, which would have helped to substantiate these findings. Such a comparison is crucial for confirming the accuracy of peak assignments in SERS data, especially when investigating substances like pesticides, where precise identification of molecular vibrations is critical. The absence of this comparison leaves a gap in the validation process of the SERS analysis conducted in the study.

Tang et al. (Tang et al., 2019) performed simultaneous SERS detection of two pesticides discussed in this review – chlorpyrifos and imidacloprid. The authors prepared a spherical SERS substrate using the silver mirror reaction on glass beads. The SERS spectra of chlorpyrifos methanolic solution with different concentrations were recorded using various concentrations under a 633 nm laser excitation. The authors achieved a chlorpyrifos LOD of 0.01 mg/L (28.5 nM). The study identified the critical vibrational modes in the chlorpyrifos SERS spectra. The most pronounced peaks were at 1097 cm^{-1} (P–O–C) and 860 cm^{-1} (C—H bending). Other less intense bands are 675 cm^{-1} (Cl—Cl stretch), 763 cm^{-1} (P–O–C stretch), 1353 cm^{-1} and 1265 cm^{-1} (Cl–ring, δ(C—H), ν_{as}(C=C), and C—H deformation). The study also provided a detailed table with the bond vibration assignments for the characteristic intensity peaks observed in the spectra of both pesticides. The peak assignment was done with respect to literature data. Moreover, the authors compared the obtained LOD with the values reached by other research groups using SERS and other methods (High-Performance Liquid Chromatography, electrochemistry, etc.). However, their approach has some limitations. For instance, the researchers did not explore the interactions between the employed SERS substrate and the pesticides, which could have provided a deeper understanding of the spectral data. This gap highlights the need for further research to fully understand the dynamics of SERS-based detection in various substrate-pesticide combinations.

Another limitation is recording SERS spectra from a narrow spectral region. For instance, many reports consider the range of 1000–1700 cm^{-1}, while chlorpyrifos has characteristic peaks in the 150–680 cm^{-1} range (see Fig. 1b). Moreover, several studies only address one or two peaks, not considering changes in other characteristic bonds. That limits our ability to compare the results, such as for the work by Park et al. (Park et al., 2022) where a unique SERS substrate was developed, drawing inspiration from biological structures and making silver nanograss (Ag–NG) to mimic the complex architecture of a lawn. The SERS experiments were performed by applying a methanolic chlorpyrifos solution with different concentrations. After drying, SERS substrates with pesticide were immersed in water for measurements under a laser excitation wavelength of 785 nm. The achieved LOD was~0.175 mg/L (500 nM). A limitation of this study was its focus on a single dominant peak at 1265 cm^{-1} in the SERS spectra. This peak became the basis for all concentration-based analyses, yet it was not linked to any specific bond in chlorpyrifos nor matched the bulk reference spectrum. Additionally, the study did not include a comparative analysis with SERS or Raman spectra from previous research on chlorpyrifos, limiting the study's conclusions.

However, a few works dedicated significant attention to detailed comparison and discussion of the experimental data. Ma et al. (Ma et al., 2020) focused on SERS detection and quantifying chlorpyrifos on tomato surfaces and extracts. The study achieved this detection thanks to an optimized silver colloid as the SERS substrate under an excitation wavelength of 638 nm. The authors obtained SERS spectra of seven different concentrations of chlorpyrifos. The observed SERS peaks are: 335 cm^{-1} (N–Cyclopropyl bending vibration); 412 cm^{-1} (P–O–C stretching); 601 cm^{-1} and 685 cm^{-1} (P═S stretching); 950 cm^{-1} (Cl-ring wagging); 1092 cm^{-1} (P–O–C stretch); 1210 cm^{-1} (Cl-ring δ(C—H) vibration); 1331 cm^{-1} (Cl-ring δ(C—H) and ν_{as}(C=C)); 1392 cm^{-1} (Cl-

ring ν(C—N) and δ(C—H)); 1439 cm^{-1} (Cl-ring ν(C=C)); and 1571 cm^{-1} (ring stretching).

The authors analyzed SERS spectra of chlorpyrifos on tomato surfaces and presented both Raman and SERS spectra of a standard chlorpyrifos solution. The SERS spectra distinctly exhibited characteristic peaks at 341, 412, 678, 975, 1278, and 1573 cm^{-1}, consistently visible across all spectra. Moreover, the intensities of these SERS peaks were directly proportional to the concentrations of the chlorpyrifos solutions.

The authors found that the SERS spectra of chlorpyrifos obtained from tomato slices matched perfectly with those measured from standard chlorpyrifos solutions. This agreement was demonstrated over a wide linear range of concentrations, from 0.001 to 1000 mg/L. Furthermore, they suggested that their method could be effectively applied to examine the surface of a whole tomato, not just the cut slices. The LOD in this case was impressively low, equal to 0.0035 mg/L (10 nM).

However, comparing the SERS spectra of chlorpyrifos, whether from standard solutions or tomato surfaces, with the Raman spectra of chlorpyrifos revealed some disparities. Notably, the relative intensities of peaks at 341, 678, and 1573 cm^{-1} observed in the Raman spectra were altered in the SERS spectra. The authors did not delve into an explanation for this variance. This change is likely associated with modifications in certain chemical bonds or the emergence of new bonds due to the interaction between the pesticide molecules and SERS substrates. Despite these unexplained discrepancies, the approach by Ma et al. (Ma et al., 2020) offers valuable insights into the application of SERS in real-world scenarios and contributes to the growing knowledge of the use of spectroscopic techniques for the analysis of pesticide residues in food products.

Another crucial work was performed by D. Zhang and co-authors (Zhang et al., 2019). The authors provided a comprehensive explanation of sample preparation, along with both normal Raman and DFT-calculated spectra for bulk chlorpyrifos. Additionally, to exclude the overlapping and overestimation, the authors included the spectrum of chlorpyrifos–methyl – a compound to which chlorpyrifos might transform under specific conditions. The bulk Raman spectrum contains all the bands seen in other works and has a clear peak assignment.

In SERS pesticide detection, the authors pinpointed the main characteristic peaks on which quantitative and qualitative analysis was built. These peaks include 679 cm^{-1} (ring breathing vibration), 750 cm^{-1} (P–O–C or P–O–R), 855 cm^{-1} (P—O stretching), 917 cm^{-1} (C—C stretching), and 1455 cm^{-1} (C—H deformation or Cl–ring and C=C stretching). Similarly to other studies, these peaks undergo shifts in SERS, which were explained by variations in the measurement environment, enhancement from the substrate, and the affinity of specific functional groups towards the substrate. EM enhancement by the substrate explains the significant enhancement of the 740 cm^{-1} band in SERS. Going beyond other works, the authors employed regression models and principal component analysis for quantitative analysis.

In the end, the authors performed SERS detection on real samples. For that, they spread the pesticide on a tea plant and let it grow for two weeks. After that, they extracted and analyzed the sample with SERS and gas chromatography-mass spectroscopy (GC–MS). The comparison between the concentrations calculated from SERS and GC–MS revealed an error of less than 20 %, which is acceptable for some analytical tasks. This work shows an excellent detection limit of ~1 ng of pesticide per 1 g of tea (Zhang et al., 2019).

Meenakshi et al. developed a graphene oxide (GO)/AuNPs nanocomposite-based SERS sensor by simply drop-casting this mixture onto a flexible parafilm substrate. The authors underlined that such a combination of materials is beneficial from several points of view. Firstly, it was expected to combine EM signal enhancement by AuNPs and CM enhancement provided by GO. Secondly, GO should promote molecular adsorption through **π-π** and electrostatic interactions. Thirdly, such a combination resulted in a hydrophobic surface, which allowed them to avoid inhomogeneous molecule distribution and coffee-ring effects. This substrate was employed to detect two pesticides, one of which was chlorpyrifos. Although the authors claimed that SERS spectra were in good agreement with literature data on Raman spectra of the pesticide, discrepancies were still noticeable and remained unaddressed in the paper. Nonetheless, using the discussed approach, the authors could detect chlorpyrifos at concentrations as low as 0.3 μM.

Another point discussed in this paper is the choice of excitation wavelength. The authors compared the effect of 532 nm and 785 nm, keeping all the other conditions the same. Parafilm substrate exhibited high luminescence under green light illumination, making the use of 785 nm optimal for a better signal (Meenakshi et al., 2023).

In a recent work by Chen et al. (Chen et al., 2023), chlorpyrifos was employed as a model molecule to investigate the impact of EM and CM enhancement on SERS signal intensity. Although the study was not primarily focused on detecting this specific pesticide, it is pertinent to discuss it within the scope of this review because they provide valuable insights into the selection of excitation wavelengths.

The authors identified that both enhancement mechanisms are crucial in SERS detection. This was tested by tuning the LSPR wavelength by adjusting proportions between Ag NPs and Ca^{2+} in the hydrogel-based SERS chips. Ca^{2+} was used to promote NP aggregation and introduce the LSPR peak position change. Furthermore, the authors considered band alignment of the tested model molecules with Fermi level of Ag clusters to investigate the CM contribution to SERS enhancement. It was found that to have the highest sensitivity (SERS intensity), the excitation wavelength should match both the LSPR position and energy difference between the Fermi level of metal and HOMO of the molecule to promote strong enhancement of confined electric field and charge transfer, respectively. In this context, for chlorpyrifos, the optimal choice of excitation wavelength was determined to be 785 nm, as the photon energy (1.58 eV) is around the energy difference between the Fermi level of Ag and the HOMO of chlorpyrifos (1.29 eV). However, in this work, the hydrogel-based SERS chip was fabricated so that the LSPR peak position also matched 785 nm, maximizing the benefits of both enhancement mechanisms. Even though the manuscript was not focused on detecting the aforementioned pesticide, the authors reported an LOD of approximately 15 nM.

Fig. 3 summarizes the most significant reports on SERS of chlorpyrifos, with SERS spectra selected to match the reference Raman spectra. Overall, this pesticide's SERS spectra appear more consistent than for malathion. The band at around 1570 cm^{-1} (C=C) has been detected in the absolute majority of the works. Typically, two peaks assigned to Cl–ring/C–H/C=C are observed between 1200 and 1360 cm^{-1}, with the Raman spectra showing two peaks at lower frequencies. Considering the consistency of these findings and the fact that the Cl– and S–locations are likely binding sites to the metallic SERS substrate, one could assume that these changes are due to molecular sorption and its different conformations (Ngo et al., 2020).

Moving forward, we focus on reviewing research reports dedicated to acquiring and analyzing imidacloprid SERS spectra.

3.3. Imidacloprid

As in the cases for malathion and chlorpyrifos, the reported results of SERS spectra for imidacloprid are also inconsistent, they often diverge from the corresponding Raman spectra of the pesticide. The main deviations and inconsistencies in these spectra and other pesticides may originate from the interaction of molecules with plasmonic SERS substrates. This may also lead to changes in molecular orbitals or the introduction of new states. Nevertheless, there are pretty detailed works where SERS spectra of imidacloprid strongly correlate with Raman spectra. For instance, one of the research works on SERS of imidacloprid was conducted by Bakar et al. (Abu Bakar and Shapter, 2023). The authors created a SERS substrate as Ag nanostars monolayers on glass. The implementation of their substrate allowed them to achieve an LOD of 1 μg/L (3.9 nM) using a 785 nm laser. Unlike many other works, SERS in

this manuscript has a surprisingly good match with Raman (see Fig. 4) and a less pronounced agreement with DFT results. Also, the authors made a detailed description of every mode (Table S1). The spectrum obtained in that work is used herein as a reference for all the works focused on the analysis of imidacloprid. The uniform nanostars distribution resulted in the reproducible SERS signal, with the highest relative standard deviation (RSD) of 16.74 %. Notably, these substrates were reusable for at least five cleaning/detection cycles.

The insufficient reliability and reproducibility of imidacloprid SERS spectra are typically accompanied by poor comparison to corresponding Raman spectra and the lack of peak assignment. In this context, the work from Zhu et al. (Zhu et al., 2021) is dedicated to the development of a novel SERS substrate by synthesizing hollow core-shell nanoflowers (NFs) composed of Au@Ag, using silver nanoparticles as a template. These nanoflowers were used to detect residues of 2,4-dichlorophenoxyacetic acid (2,4D) and imidacloprid. The SERS and Raman spectra for imidacloprid residues in milk were obtained under 785 nm excitation wavelength, with a LOD for imidacloprid of 0.055 mg/L (21.5 nM). The authors observed that the most prominent peaks in the SERS spectra for imidacloprid appeared at 815 cm^{-1} and 995 cm^{-1}. They also identified additional spectral features at 632, 752, 1276, 1371, and 1584 cm^{-1} being coherent with Raman obtained by the reference work (Abu Bakar and Shapter, 2023). However, the study should have addressed the specifics or provided assignments for the peaks in the imidacloprid spectra. This lack of detailed peak assignments contrasts with their analysis of 2,4D, where the authors explained and assigned the vibrational modes corresponding to the most prominent peaks. Additionally, the study did not include any direct comparative analysis with SERS spectra of milk or with previously reported imidacloprid SERS spectra, which could be especially useful in complex matrices like food products.

In their innovative research, Pham et al. (Pham et al., 2022) developed a SERS substrate inspired by the complex structure of rose petals, using a PDMS elastomer base and Ag/AgNPs coating. The study showed the acquisition of Raman and SERS spectra at 633 nm wavelength for various forms of imidacloprid, including powder, solutions, and residues

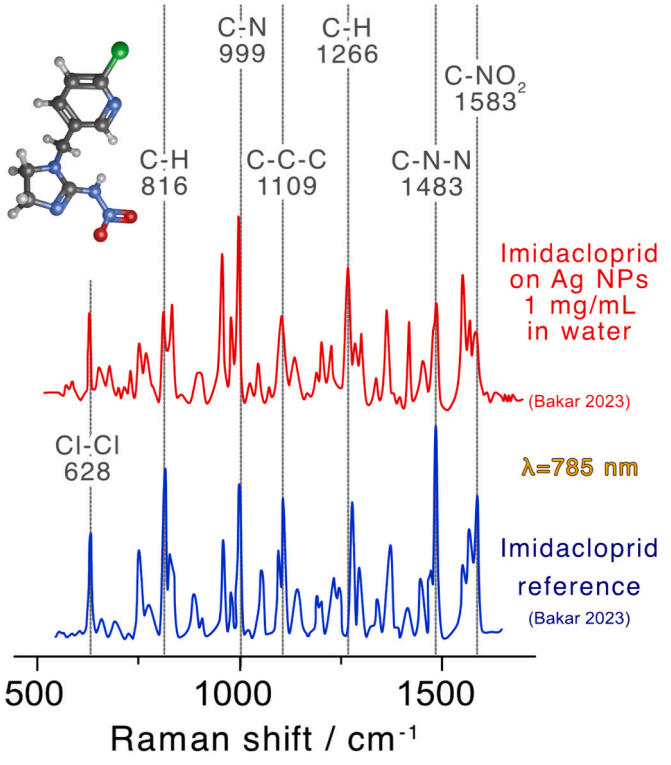

Fig. 4. Representative Raman and SERS spectra of imidacloprid with peak assignments from Bakar et al. (Abu Bakar and Shapter, 2023).

in mango fruit, as well as for other pesticides. The LOD for imidacloprid was 0.02 mg/kg or ~ 0.002 mg/L (7.82 nM). The characteristic Raman peaks for imidacloprid were 660 cm^{-1} (C—Cl stretching), 830 cm^{-1} and 1110 cm^{-1} (C–C–C bonds), 989 cm^{-1} and 1351 cm^{-1} (C—N stretching). Those peaks in the SERS spectrum of a standard imidacloprid solution were observed at 829 cm^{-1}, 959 cm^{-1}, 993 cm^{-1}, and 1105 cm^{-1}. The authors observed that the peaks corresponding to imidacloprid in mango extracts closely matched those in reference solutions. Additionally, a positive correlation was observed between the intensity of imidacloprid peaks and their concentration, spanning from 0.01 to 100.00 mg/kg. Interestingly, the peak at 1105 cm^{-1} maintained its position, while peaks around 800 cm^{-1}, 1365 cm^{-1}, and 1574 cm^{-1} were shifted, possibly due to interactions between imidacloprid and the AgNPs. Some of the peaks match well with the representative Raman spectrum. Although a direct comparison with previous research on imidacloprid spectra was not presented, the authors provided both Raman and SERS spectra. Furthermore, they included a Raman spectrum of mango, which allowed a more comprehensive evaluation of their results. This addition was crucial for understanding the potential impact of the matrix on the SERS spectra and for assessing the specificity of the substrate in detecting imidacloprid in complex biological matrices.

In another study by Chen et al. (Chen et al., 2019), Ag NFs were used as the SERS substrate for analyzing imidacloprid residues in green tea, using a 785 nm laser excitation wavelength. The researchers presented both the Raman and SERS spectra of imidacloprid with its concentration levels in green tea. The LOD achieved with this method was 0.1 μg/L (0.39 nM). The study noted an increase in SERS intensity proportional to the concentration of imidacloprid. A consistent characteristic peak at 660 cm^{-1} (C—Cl stretching) was observed across various concentrations. Additional peaks at 1351 and 1580 cm^{-1} were assigned to the symmetric and asymmetric C–NO_2 vibrations, respectively. However, not all the visible peaks in the spectra were assigned to specific bonds.

In the research by Tang et al. (Tang et al., 2019), which was cited in the previous subchapter dedicated to chlorpyrifos, SERS spectra of imidacloprid revealed a LOD of 0.05 mg/L (0.2 μM). The authors observed that while the SERS spectra on the non-planar substrate showed slight fluorescence, one of the imidacloprid peaks was still distinguishable at 1397 cm^{-1} (Cl–ring) and used for quantification. Other SERS peaks are 824 cm^{-1} (out-of-plane C—H bending), 878 cm^{-1} (N—O stretching), 1039 cm^{-1} (N—O stretching), 1096 cm^{-1} (in-plane C—H bending), and 1169 cm^{-1} (C—N stretching). The authors compared peak assignment to previous reports and underlined the consistency and appearance of the peak at 878 cm^{-1} (N—O stretching), which was not reported elsewhere. However, these spectra do not show a good match with the Raman spectrum of imidacloprid.

There are studies in which the authors suggest possible reasons for the discrepancies mentioned above between the Raman and SERS spectra of imidacloprid, as well as for the shifts of some characteristic peaks. Among such studies is the work by Al-Syadi et al.(Al-Syadi et al., 2021), where a novel approach for SERS substrate development was proposed. The substrate represented porous silicon (PSi) decorated with layers of palladium nanoparticles (Pd NPs). This study involved recording both Raman spectra on PSi and SERS spectra on PSi-Pd NPs for an imidacloprid solution under a 785 nm laser excitation. The research successfully demonstrated an LOD of 2.56 μg/L (10 nM). Characteristic peak assignments for imidacloprid under both normal Raman/SERS conditions were discussed in the paper. The authors documented the shift between Raman and SERS spectra; however, they did not dig much into its origin. These included peaks at 316/302 cm^{-1} (N–C–N bond out-of-plane), 817/800 cm^{-1} (C—H in-plane rocking), 989/947 cm^{-1} (C—N stretching), 1273/1245 cm^{-1} (N—N stretching), 1363/1352 cm^{-1} (C—N stretching), and 1555/1562 cm^{-1} (C—H in-plane bending). The study observed that the PSi-Pd NPs substrates displayed more intense peaks compared to bare PSi substrates, along with slight shifts in peak positions. This enhancement occurred since nanocrystallites acted as “hot spots” generated at the junctions between different surface

components of the substrate or among the Pd NPs within the PSi substrates. The high surface area and the dense packing of nanoparticles within the PSi-Pd NPs substrate contributed to the efficient generation of these "hot spots," thus enhancing the SERS effect.

Another good example is the research by Creedon et al. (Creedon et al., 2020), where a nanostructured silver-coated polyvinylidene fluoride (PVDF) substrate was employed for SERS. The authors obtained SERS spectra of imidacloprid and conducted comparative analyses with normal Raman and DFT-calculated spectra, as was done by Bakar et al. (Abu Bakar and Shapter, 2023). The SERS and Raman measurements were performed in a methanol–deionized water solution under a 514 nm excitation wavelength, achieving a low LOD of 1 μg/L (3.9 nM). The study provided a thorough analysis of the obtained SERS spectra, assigning specific vibrational modes to each observed peak. Key peak assignments included multiple in-plane rocking modes involving C—H at 815 cm^{-1}, 751 cm^{-1}, and 691 cm^{-1}; the stretching mode of N − N at 1241 cm^{-1}; in-plane bending vibrations of C—H at 1277 cm^{-1}, 1371 cm^{-1}, and 1451 cm^{-1}; and symmetric and asymmetric stretching vibrations of N − O at 1302 cm^{-1} and 1584 cm^{-1}. The authors noted significant differences between the SERS and conventional Raman spectra, particularly in terms of relative intensities and peak shifts. They hypothesized that these variations could be linked to the way the molecule interacts with the substrate surface. According to their explanation, it is a well-established concept that the adsorption of molecules onto a surface can alter their energy levels. Such alterations perturb the vibrational modes of the molecules, resulting in shifts in peak positions and variations in peak intensities. This study provides valuable insights into the impact of molecular adsorption on SERS spectra and enhances the understanding of how surface interactions can influence spectroscopic characterizations. Such dependence of Raman peaks in SERS according to the molecular orientation has been previously discussed by Rodriguez et al. (Rodriguez et al., 2021).

One of the most recent works on imidacloprid by Cai et al. performed a well-executed SERS analysis of imidacloprid in tap and lake water samples. At first, the reference experiments were conducted in distilled water to identify spectral patterns of the pesticide molecule that could be used further for analysis (Cai et al., 2023). The authors could identify imidacloprid spectral patterns at concentrations ranging from 100 to 0.1 μM in tap water, however, the spectra did not demonstrate sufficient reproducibility. One of the reasons behind this inconsistency was attributed to poor agglomeration of colloidal Au NPs (SERS substrate), which resulted in inhomogeneous enhancement. This issue was solved by introducing an agglomeration agent – K_2SO_4, which led to more pronounced enhancement and excellent reproducibility of spectra. However, for concentrations below 0.1 μM, the spectra were found to be dominated by the sodium citrate band (a compound used as a capping agent during NPs synthesis). Such behavior was explained by the competitive adsorption of sodium citrate and imidacloprid on the Au NPs surface. Thus, the high concentrations of imidacloprid could successfully displace citrate molecules to provide an SERS signal. The orientation and distance from the "hot spots" also played a crucial role in SERS enhancement, resulting in a poor signal at low concentrations. Using SERS detection, the authors got a LOD of 0.1 μM.

Further, the authors implemented a "citrate background" subtraction, coupled with multivariable analysis techniques to enhance the analytical capabilities of their approach. Such methods include principal component analysis, SERS barcoding, and vector angle calculation. Together, these processing methods allowed LOD to drop to an impressive value of 1 nM. Such LOD is eight times lower than the guideline set by the Minnesota Department of Health and 1–2 orders of magnitude higher than LODs of LC-MS/MS. This SERS platform was proposed as a prescreening sensor to raise an alarm that the concentration of imidacloprid is higher than the guideline for drinking water.

Fig. 4 summarizes the SERS peak positions reported for imidacloprid, with a representative Raman spectrum and a SERS spectrum selected for closely matching the Raman spectrum. The reference Raman spectrum in Bakar's work matches other reports, as shown by the comparison in Fig. S2. In summary, imidacloprid Raman spectra are extremely rich in well-defined features. In contrast, in most cases, SERS spectra present broader peaks and fewer features that can still be interpreted as imidacloprid peaks. For most of the work, it was observed that SERS spectra deviate from the Raman ones in the way that peaks are getting broader with significant shifts in their positions (up to 40 cm^{-1}). Moreover, in some works, we noticed the appearance of two broad bands in the range 1200–1600 cm^{-1}), which might be an indication of experimental conditions leading to a substance burning, resulting in the formation of carbonaceous species.

4. Summary and discussion

This manuscript has undertaken an in-depth review of the advancements and applications of SERS in pesticide detection, focusing on some of the key pesticides such as malathion, chlorpyrifos, and imidacloprid. The analysis of various studies reveals the exceptional capabilities of SERS in detecting ultralow concentrations of these pesticides, which is crucial for ensuring environmental safety and food security. The highlighted studies demonstrated the versatility of SERS, particularly in terms of its ability to require minimal sample preparation, thereby making it a suitable and efficient tool for various applications, including in-situ field analyses and rapid screening processes.

One of the significant findings from the reviewed literature is the development of innovative SERS substrates. These include complex nanostructures, such as silver nanostructures and hybrid gold-silver nanoflowers, which have been shown to significantly enhance the Raman signal, allowing more precise and accurate pesticide detection. These novel substrates have led to the development of highly sensitive SERS setups capable of detecting pesticides at concentrations lower than the permissible limits. This high sensitivity highlights the potential of SERS in revolutionizing the detection and monitoring of pesticide residues in various environments and food products.

In addition to the sensitivity of SERS, the studies have also shown its applicability in real-world scenarios. The technique's ability to detect multiple pesticides simultaneously is remarkable. This aspect of SERS is particularly advantageous in agriculture analyses where the simultaneous presence of multiple pesticide residues is a common occurrence.

However, this review also highlights some limitations in the interpretation of SERS spectra. While some studies demonstrate a close correspondence between the SERS and Raman features, others show significant differences both from Raman spectra and from other reported SERS spectra. This variability in the data emphasizes the need for a more elaborated understanding of the interaction between the SERS substrates and the pesticide molecules. The studies suggest that the adsorption of pesticide molecules onto various substrates can change their energy states and vibrational modes, leading to shifts in peak positions and changes in relative peak intensities. Chemical transformations from binding to decomposition in the "hot spots" add additional complexity to the data interpretation. These findings highlight the complex nature of SERS and the factors that can influence the outcomes of such studies, such as chemical transformations and changes in the bond polarizability.

Moreover, current research presents a substantial degree of variability and discrepancies in the data reported (see Table S1), which poses challenges in drawing definitive conclusions. These inconsistencies across different studies call for more standardized methodologies and rigorous comparative analyses. Such efforts are essential for validating the reliability and applicability of SERS in pesticide detection and ensuring that the research contributes meaningfully to the broader scientific community and practical applications.

In conclusion, while SERS exhibits immense potential in pesticide detection, realizing this potential fully requires addressing the highlighted methodological and interpretation challenges. The future of SERS in pesticide detection looks promising, with opportunities for

significant contributions to environmental monitoring and food safety, provided these challenges are systematically addressed in ongoing and future research.

5. Challenges and prospects of SERS in pesticide detection

While SERS has shown great promise in detecting pesticides, there are several critical challenges to be addressed in future research. Solving these bottlenecks is crucial in establishing SERS as a reliable tool in environmental and food safety applications.

5.1. Standardization of experimental protocols

A significant drawback in SERS research is the need for uniformity in experimental approaches. To reproduce and compare the data for drawing reliable conclusions, the experimental details must include not only the basic parameters such as Raman spectroscopy measurement details (e.g., laser wavelength, power, focusing and collection optics, and spectral resolution), source and purity of chemicals, and substrate preparation procedure but also the method of pesticide deposition including the duration of the sorption, pesticide's physical state during the measurements (solid or liquid), relevant statistics (how many points have been measured).

The reference data must necessarily include bulk Raman reference, spectra of control blank SERS substrate prepared exactly the same way as the pesticide sample (e.g., immersed in the solvent without the pesticide). For some reported data, the background consisting of D and G peaks is observed, which means that there is a risk of the analyte decomposition. Therefore, in such cases power-dependent measurements should also be reported to confirm the signal stability. Concentration dependence is also a meaningful way to verify experimental validity.

One more not obvious aspect of SERS in pesticide detection is that most works we reviewed used near-infrared laser excitation at 780 or 785 nm, with a few works using red and exceptionally green lasers, while the plasmonic nanostructures show resonances in the visible blue-green range. Indeed, SERS spectra can also be obtained under non-resonant conditions, and the type of system under study may determine the use of lasers at other wavelengths outside of resonance. In fact, for silver-based structures, choosing a 785 nm laser might promote CM enhancement (Y. Liu et al., 2022). Indeed CM enhancement may be another mechanism affecting spectral changes. However, it was shown that to achieve optimal signal enhancement in this scenario, the SERS substrate should be engineered so that the 785 nm excitation wavelength matches the LSPR position. With this alignment, it remains to be seen whether matching the laser with the LSPR would result in improved signal quality and high sensitivity. Based on this, there appears to be space for optimizing the SERS signal intensity by simply matching the laser excitation energy to both the LSPR of the plasmonic nanostructures and charge transfer, resulting in the largest signal enhancement. (Merlen et al., 2010; Meyer et al., 2011) This point deserves a closer look in future work by performing multi-wavelength SERS investigations of different pesticides and determining if the lack of unified SERS spectra could be related to this laser wavelength/LSPR mismatch.

5.2. SERS substrate fabrication

To ensure high-quality data, it is important to fabricate substrates with a uniform distribution of "hot spots" along their surface and provide the data on the substrate uniformity. In addition to accumulating SERS statistics, it is meaningful to employ various techniques for nano and microscale analysis, including scanning electron microscopy (SEM) and atomic force microscopy (AFM). These complementary techniques are crucial for assessing the surface morphology that defines homogeneity and configuration of "hot spots". In colloidal systems, this can be achieved by introducing agglomeration agents (Ge et al., 2022), while films present greater challenges that require new experimental designs in the future.

Additionally, predicting the surface/molecule interactions might help to develop more suitable substrates for SERS detection. For example, in the case of malathion or imidacloprid, superhydrophobic substrates could promote adsorption, thus facilitating the acquisition of more reliable data.

5.3. Spectral analysis range

The range of Raman shifts analyzed in many studies is often limited, potentially overlooking other relevant vibrational modes associated with pesticide molecules. Expanding the range of analysis can reveal additional spectral features that might be critical for identifying and differentiating pesticides. We propose to always include the spectral range from 300 to 1800 cm^{-1}, where the main vibrations of pesticides occur.

5.4. Spectral analysis

First of all, it is crucial to report the processing used and use smoothing and other spectral modification tools cautiously. When identifying the peaks, the authors should exercise a consistent approach: list all the peaks observed even if they cannot be assigned, explicitly mark any parasitic signals, such as substrate or solvent features, and avoid assigning peaks that are comparable to the noise level. A persistent gap in current research is insufficiently comparing new SERS spectral data with established reference spectra. Such comparative analysis is essential for validating new findings and understanding the influence of different experimental conditions on spectral characteristics, and providing a more robust framework for interpreting new data. This includes transparently reporting the observed shifts and intensity changes considering multiple sources.

Moreover, statistical and machine learning methods have shown significant potential for spectral analysis and error minimization. These methods have already been implemented as multivariable analysis (Cai et al., 2023; Zhang et al., 2019).

5.5. In-depth analysis of SERS substrate-pesticide interactions

While many studies acknowledge the influence of substrate-pesticide interactions on SERS spectra, there needs to be more in-depth analysis of these interactions. Future research should focus on how different materials of SERS substrates (such as silver or gold nanoparticles) interact with various pesticides. This understanding is crucial for accurately interpreting spectral data and tailoring substrate design for specific pesticide detection. The typical issues of the SERS substrates that must be solved are inhomogeneity, sensitivity, and multiplex detection capability (Fan et al., 2020; Liu et al., 2021; Mosier-Boss, 2017; Ouyang et al., 2017). In such complex systems as pesticides and their mixtures, being able to compare the data from different works directly is extremely important. Here, using standard substrates as a reference and providing raw data along with the paper would greatly help get maximum value from work performed by the scientific community pushing SERS in environmental applications.

By addressing these challenges, future research in SERS can advance towards developing more reliable and precise techniques for pesticide detection, ultimately contributing to safer environmental and food practices.

CRediT authorship contribution statement

Andrey Averkiev: Methodology, Visualization, Writing – original draft, Writing – review & editing. **Raul D. Rodriguez:** Visualization, Writing – review & editing. **Maxim Fatkullin:** Conceptualization, Formal analysis, Writing – review & editing. **Anna Lipovka:** Formal

analysis, Writing – review & editing. **Bin Yang:** Writing – review & editing. **Xin Jia:** Writing – review & editing. **Olfa Kanoun:** Funding acquisition, Writing – review & editing. **Evgeniya Sheremet:** Conceptualization, Funding acquisition, Project administration, Supervision, Writing – review & editing.

Declaration of competing interest

The authors declare that they have no known competing financial interests or personal relationships that could have appeared to influence the work reported in this paper.

Data availability

Data will be made available on request.

Acknowledgments

This work was supported by RFBR and DFG grant, project number 21-53-12045, Natural Science Foundation of China (22308223), and the Agrochemical Engineering Innovation and Intelligence Base for Oasis Ecology.

Appendix A. Supplementary data

Supplementary data to this article can be found online at https://doi.org/10.1016/j.scitotenv.2024.173262.

References

Abu Bakar, N., Shapter, J.G., 2023. Silver nanostar films for surface-enhanced Raman spectroscopy (SERS) of the pesticide imidacloprid. Heliyon 9, e14686.
Alavanja, M.C.R., 2009. Introduction: pesticides use and exposure extensive worldwide. Rev. Environ. Health 24, 303–309.
Alavanja, M.C.R., Bonner, M.R., 2012. Occupational pesticide exposures and cancer risk: a review. J. Toxicol. Environ. Health B Crit. Rev. 15, 238–263.
Alexandratos, N., Bruinsma, J., Alexandratos, N., Bruinsma, J., 2012. World agriculture towards 2030/2050: the 2012 revision. https://doi.org/10.22004/AG.ECON.288998.
Al-Syadi, A.M., Faisal, M., Harraz, F.A., Jalalah, M., Alsaiari, M., 2021. Immersion-plated palladium nanoparticles onto meso-porous silicon layer as novel SERS substrate for sensitive detection of imidacloprid pesticide. Sci. Rep. 11, 9174.
Asgari, S., Wu, G., Aghvami, S.A., Zhang, Y., Lin, M., 2021. Optimisation using the finite element method of a filter-based microfluidic SERS sensor for detection of multiple pesticides in strawberry. Food Addit. Contam. Part a Chem. Anal. Control Expo. Risk Assess. 38, 646–658.
Bakirhan, N.K., Uslu, B., Ozkan, S.A., 2018. The detection of pesticide in foods using electrochemical sensors. Food Safety and Preservation Elsevier 91–141.
Benitta T, A., Kapoor, S., Christy R, S., Sobana Raj C, I., Thanka Kumaran J, T., 2017. Surface enhanced Raman spectra and theoretical study of an organophosphate malathion. Orient. J. Chem. 33, 760–767.
Bernat, A., Samiwala, M., Albo, J., Jiang, X., Rao, Q., 2019. Challenges in SERS-based pesticide detection and plausible solutions. J. Agric. Food Chem. 67, 12341–12347.
Cai, S., Cho, S.W., Wei, H., 2023. Rapid prescreening of trace imidacloprid in drinking water via concentration-dependent surface-enhanced Raman spectroscopic patterns. ACS ES T Eng 3, 1875–1885.
Carvalho, F.P., 2017. Pesticides, environment, and food safety. Food Energy Secur. 6, 48–60.
Chen, M., Liu, Z., Su, B., Hu, R., Fu, F., Jiang, X., Lin, Z., Dong, Y., 2023. High-performance hydrogel SERS chips with tunable localized surface plasmon resonance for coordinated electromagnetic enhancement with chemical enhancement. Adv. Opt. Mater. 11 https://doi.org/10.1002/adom.202202852.
Chen, Q., Hassan, M.M., Xu, J., Zareef, M., Li, H., Xu, Y., Wang, P., Agyekum, A.A., Kutsanedzie, F.Y.H., Viswadevarayalu, A., 2019. Fast sensing of imidacloprid residue in tea using surface-enhanced Raman scattering by comparative multivariate calibration. Spectrochim. Acta A Mol. Biomol. Spectrosc. 211, 86–93.
Chen, Y., Liu, L., Xu, L., Song, S., Kuang, H., Cui, G., Xu, C., 2017. Gold immunochromatographic sensor for the rapid detection of twenty-six sulfonamides in foods. Nano Res. 10, 2833–2844.
Creedon, N., Lovera, P., Moreno, J.G., Nolan, M., O'Riordan, A., 2020. Highly sensitive SERS detection of neonicotinoid pesticides. Complete Raman spectral assignment of Clothianidin and Imidacloprid. J. Phys. Chem. A 124, 7238–7247.
Dias, L.A.F., Jussiani, E.I., Appoloni, C.R., 2019. Reference Raman spectral database of commercial pesticides. J. Appl. Spectrosc. 86, 166–175.
Fan, M., Andrade, G.F.S., Brolo, A.G., 2020. A review on recent advances in the applications of surface-enhanced Raman scattering in analytical chemistry. Anal. Chim. Acta 1097, 1–29.
Fathi, F., Lagugné-Labarthet, F., Pedersen, D.B., Kraatz, H.-B., 2012. Studies of the interaction of two organophosphonates with nanostructured silver surfaces. Analyst 137, 4448–4453.
Ge, H., Yin, R., Su, P., Yu, L., Lei, M., Sun, M., Sun, Z., Wang, S., 2022. On-site detection of As(III) based on silver nanoparticles aggregation mediated by phosphates using surface-enhanced Raman scattering (SERS). Mikrochim. Acta 189, 44.
Jia, K., Xie, J., He, X., Zhang, D., Hou, B., Li, X., Zhou, X., Hong, Y., Liu, X., 2020. Polymeric micro-reactors mediated synthesis and assembly of ag nanoparticles into cube-like superparticles for SERS application. Chem. Eng. J. 395, 125123.
Jiang, L., Hassan, M.M., Ali, S., Li, H., Sheng, R., Chen, Q., 2021. Evolving trends in SERS-based techniques for food quality and safety: a review. Trends Food Sci. Technol. 112, 225–240.
Kaur, N., Khunger, A., Wallen, S.L., Kaushik, A., Chaudhary, G.R., Varma, R.S., 2021. Advanced green analytical chemistry for environmental pesticide detection. Curr. Opin. Green Sustain. Chem. 30, 100488.
Kulakovich, O.S., Matsukovich, A.S., Trotsiuk, L.L., 2022. Challenges in surface-enhanced Raman scattering detection of pesticide carbendazim and ways to overcome. J. Nanophot. 16 https://doi.org/10.1117/1.jnp.16.046002.
Li, H., Hassan, M.M., He, Z., Haruna, S.A., Chen, Q., Ding, Z., 2022. A sensitive silver nanoflower-based SERS sensor coupled novel chemometric models for simultaneous detection of chlorpyrifos and carbendazim in food. Lebenson. Wiss. Technol. 167, 113804.
Li, Y., Sun, Y., Peng, Y., Dhakal, S., Chao, K., Liu, Q., 2012. Rapid detection of pesticide residue in apple based on Raman spectroscopy, in: sensing for agriculture and food quality and safety IV. Presented at the SPIE Defense, Security, and Sensing, SPIE. https://doi.org/10.1117/12.918527.
Liang, X., Li, L., Han, C., Dong, Y., Xu, F., Lv, Z., Zhang, Y., Qu, Z., Dong, W., Sun, Y., 2022. Rapid limit test of seven pesticide residues in tea based on the combination of TLC and Raman imaging microscopy. Molecules 27. https://doi.org/10.3390/molecules27165151.
Lin, Z., He, L., 2019. Recent advance in SERS techniques for food safety and quality analysis: a brief review. Curr. Opin. Food Sci. 28, 82–87.
Liu, C., Xu, D., Dong, X., Huang, Q., 2022. A review: research progress of SERS-based sensors for agricultural applications. Trends Food Sci. Technol. 128, 90–101.
Liu, H., He, Y., Cao, K., 2021. Flexible surface-enhanced Raman scattering substrates: a review on constructions, applications, and challenges. Adv. Mater. Interfaces 8, 2100982.
Liu, Y., Liu, T., 2011. Determination of pesticide residues on the surface of fruits using micro-Raman spectroscopy. In: Computer and Computing Technologies in Agriculture IV. Springer, Berlin Heidelberg, Berlin, Heidelberg, pp. 427–434.
Liu, Y., Zhang, L., Liu, X., Zhang, Y., Yan, Y., Zhao, Y., 2022. In situ SERS monitoring of plasmon-driven catalytic reaction on gap-controlled Ag nanoparticle arrays under 785 nm irradiation. Spectrochim. Acta A Mol. Biomol. Spectrosc. 270, 120803.
Ma, P., Wang, L., Xu, L., Li, J., Zhang, X., Chen, H., 2020. Rapid quantitative determination of chlorpyrifos pesticide residues in tomatoes by surface-enhanced Raman spectroscopy. Eur. Food Res. Technol. 246, 239–251.
Meenakshi, M.M., Annasamy, G., Sankaranarayanan, M., 2023. Highly sensitive technique for detection of adulterants in centella herbal samples using surface enhanced Raman spectroscopy (SERS). Spectrochim. Acta A Mol. Biomol. Spectrosc. 299, 122878.
Merlen, A., Lagugné-Labarthet, F., Harté, E., 2010. Surface-enhanced Raman and fluorescence spectroscopy of dye molecules deposited on nanostructured gold surfaces. J. Phys. Chem. C. Nanomater. Interfaces 114, 12878–12884.
Meyer, S.A., Le Ru, E.C., Etchegoin, P.G., 2011. Combining surface plasmon resonance (SPR) spectroscopy with surface-enhanced Raman scattering (SERS). Anal. Chem. 83, 2337–2344.
Mitra, C.K., Sharma, M.D., Ghosh, M., Pande, S., Chowdhury, J., 2024. Gold Nano-colloids impregnated in Langmuir-Blodgett film of MoS2 flakes as SERS active platform: fabrication and its application in malathion detection. Curr. Appl. Phys. 63, 18–31.
Moldovan, R., Iacob, B.-C., Farcău, C., Bodoki, E., Oprean, R., 2021. Strategies for SERS detection of organochlorine pesticides. Nanomaterials (Basel) 11. https://doi.org/10.3390/nano11020304.
Mosier-Boss, P.A., 2017. Review of SERS substrates for chemical sensing. Nanomaterials (Basel) 7. https://doi.org/10.3390/nano7060142.
Narenderan, S.T., Meyyanathan, S.N., Babu, B., 2020. Review of pesticide residue analysis in fruits and vegetables. Pre-treatment, extraction and detection techniques. Food Res. Int. 133, 109141.
Nazarloo, A.S., Sharabiani, V.R., Gilandeh, Y.A., Taghinezhad, E., Szymanek, M., 2021. Evaluation of Different Models for Non-Destructive Detection of Tomato Pesticide Residues Based on Near-Infrared Spectroscopy. Sensors 21. https://doi.org/10.3390/s21093032.
Ngo, T.C., Trinh, Q.T., Thi Thai An, N., Tri, N.N., Trung, N.T., Truong, D.H., Huy, Bui The, Nguyen, M.T., Dao, D.Q., 2020. SERS spectra of the pesticide chlorpyrifos adsorbed on silver nanosurface: the Ag_{20} cluster model. J. Phys. Chem. C. Nanomater. Interfaces 124, 21702–21716.
Nie, Y., Teng, Y., Li, P., Liu, W., Shi, Q., Zhang, Y., 2018. Label-free aptamer-based sensor for specific detection of malathion residues by surface-enhanced Raman scattering. Spectrochim. Acta A Mol. Biomol. Spectrosc. 191, 271–276.
Ouyang, L., Ren, W., Zhu, L., Irudayaraj, J., 2017. Prosperity to challenges: recent approaches in SERS substrate fabrication. Rev. Anal. Chem. 36 https://doi.org/10.1515/revac-2016-0027.
Pang, S., Yang, T., He, L., 2016. Review of surface enhanced Raman spectroscopic (SERS) detection of synthetic chemical pesticides. Trends Anal. Chem. 85, 73–82.
Park, H., Park, J., Lee, G., Kim, W., Park, J., 2022. Detection of Chlorpyrifos using bio-inspired silver Nanograss. Materials 15. https://doi.org/10.3390/ma15103454.

Pham, U.T., Phan, Q.H.T., Nguyen, L.P., Luu, P.D., Doan, T.D., Trinh, H.T., Dinh, C.T., Van Nguyen, T., Tran, T.Q., Le, D.X., Pham, T.N., Le, T.D., Nguyen, D.T., 2022. Rapid quantitative determination of multiple pesticide residues in mango fruits by surface-enhanced Raman spectroscopy. Processes (Basel) 10, 442.

Qu, C., Albanese, S., Lima, A., Hope, D., Pond, P., Fortelli, A., Romano, N., Cerino, P., Pizzolante, A., De Vivo, B., 2019. The occurrence of OCPs, PCBs, and PAHs in the soil, air, and bulk deposition of the Naples metropolitan area, southern Italy: implications for sources and environmental processes. Environ. Int. 124, 89–97.

Quintás, G., Garrigues, S., de la Guardia, M., 2004. FT-Raman spectrometry determination of malathion in pesticide formulations. Talanta 63, 345–350.

Richendrfer, H., Creton, R., 2015. Chlorpyrifos and malathion have opposite effects on behaviors and brain size that are not correlated to changes in AChE activity. Neurotoxicology 49, 50–58.

Rodriguez, R.D., Villagómez, C.J., Khodadadi, A., Kupfer, S., Averkiev, A., Dedelaite, L., Tang, F., Khaywah, M.Y., Kolchuzhin, V., Ramanavicius, A., Adam, P.-M., Gräfe, S., Sheremet, E., 2021. Chemical enhancement vs molecule–substrate geometry in plasmon-enhanced spectroscopy. ACS Photonics 8, 2243–2255.

Serebrennikova, K.V., Komova, N.S., Aybush, A.V., Zherdev, A.V., Dzantiev, B.B., 2023. Flexible substrate of cellulose Fiber/structured Plasmonic silver nanoparticles applied for label-free SERS detection of malathion. Materials 16. https://doi.org/10.3390/ma16041475.

Song, E., Yu, M., Wang, Y., Hu, W., Cheng, D., Swihart, M.T., Song, Y., 2015. Multi-color quantum dot-based fluorescence immunoassay array for simultaneous visual detection of multiple antibiotic residues in milk. Biosens. Bioelectron. 72, 320–325.

Starner, K., Goh, K.S., 2012. Detections of the neonicotinoid insecticide imidacloprid in surface waters of three agricultural regions of California, USA, 2010-2011. Bull. Environ. Contam. Toxicol. 88, 316–321.

Tang, J., Chen, W., Ju, H., 2019. Rapid detection of pesticide residues using a silver nanoparticles coated glass bead as nonplanar substrate for SERS sensing. Sensors Actuators B Chem. 287, 576–583.

Tsagkaris, A.S., Pulkrabova, J., Hajslova, J., 2021. Optical screening methods for pesticide residue detection in food matrices: advances and emerging analytical trends. Foods 10. https://doi.org/10.3390/foods10010088.

Valdovinos-Flores, C., Alcantar-Rosales, V.M., Gaspar-Ramírez, O., Saldaña-Loza, L.M., Dorantes-Ugalde, J.A., 2017. Agricultural pesticide residues in honey and wax combs from southeastern, central and northeastern Mexico. J. Apic. Res. 56, 667–679.

Vasseghian, Y., Dragoi, E.-N., Almomani, F., Golzadeh, N., Vo, D.-V.N., 2022. A global systematic review of the concentrations of malathion in water matrices: Meta-analysis, and probabilistic risk assessment. Chemosphere 291, 132789.

Wang, L., Cai, J., Wang, Y., Fang, Q., Wang, S., Cheng, Q., Du, D., Lin, Y., Liu, F., 2014. A bare-eye-based lateral flow immunoassay based on the use of gold nanoparticles for simultaneous detection of three pesticides. Mikrochim. Acta 181, 1565–1572.

Wu, H., Zhang, R., Liu, J., Guo, Y., Ma, E., 2011. Effects of malathion and chlorpyrifos on acetylcholinesterase and antioxidant defense system in Oxya chinensis (Thunberg) (Orthoptera: Acrididae). Chemosphere 83, 599–604.

Xu, M.-L., Gao, Y., Han, X.X., Zhao, B., 2017. Detection of pesticide residues in food using surface-enhanced Raman spectroscopy: a review. J. Agric. Food Chem. 65, 6719–6726.

Xu, R., Dai, S., Dou, M., Yang, J., Wang, X., Liu, X., Wei, C., Li, Q., Li, J., 2023. Simultaneous, Label-Free and High-throughput SERS Detection of Multiple Pesticides on Ag@Three-Dimensional Silica Photonic Microsphere Array. J. Agric. Food Chem. 71, 3050–3059.

Yu, X., Zhang, X., Wang, Z., Jiang, H., Lv, Z., Shen, J., Xia, G., Wen, K., 2018. Universal simultaneous multiplex ELISA of small molecules in milk based on dual luciferases. Anal. Chim. Acta 1001, 125–133.

Zhai, W., Cao, M., Xiao, Z., Li, D., Wang, M., 2022. Rapid detection of malathion, Phoxim and Thiram on Orange surfaces using ag nanoparticle modified PDMS as surface-enhanced Raman spectroscopy substrate. Foods 11. https://doi.org/10.3390/foods11223597.

Zhang, D., Liang, P., Ye, J., Xia, J., Zhou, Y., Huang, J., Ni, D., Tang, L., Jin, S., Yu, Z., 2019. Detection of systemic pesticide residues in tea products at trace level based on SERS and verified by GC-MS. Anal. Bioanal. Chem. 411, 7187–7196.

Zhang, D., Liang, P., Chen, W., Tang, Z., Li, C., Xiao, K., Jin, S., Ni, D., Yu, Z., 2021. Rapid field trace detection of pesticide residue in food based on surface-enhanced Raman spectroscopy. Mikrochim. Acta 188, 370.

Zhu, A., Xu, Y., Ali, S., Ouyang, Q., Chen, Q., 2021. Au@ag nanoflowers based SERS coupled chemometric algorithms for determination of organochlorine pesticides in milk. Lebenson. Wiss. Technol. 150, 111978.

Zhu, J., Agyekum, A.A., Kutsanedzie, F.Y.H., Li, H., Chen, Q., Ouyang, Q., Jiang, H., 2018. Qualitative and quantitative analysis of chlorpyrifos residues in tea by surface-enhanced Raman spectroscopy (SERS) combined with chemometric models. Lebenson Wiss Technol 97, 760–769.

Zhu, J., Ahmad, W., Xu, Y., Liu, S., Chen, Q., Hassan, M.M., Ouyang, Q., 2019. Development of a novel wavelength selection method for the trace determination of chlorpyrifos on au@ag NPs substrate coupled surface-enhanced Raman spectroscopy. Analyst 144, 1167–1177.